

引用格式: WANG Haizhen, CHENG Xue, LIN Tinghao, et al. Optical Anisotropy of One-dimensional Double Chain  $C_5H_{16}N_2Pb_2I_6$  Perovskites (Invited)[J]. Acta Photonica Sinica, 2023, 52(3):0352111

王海珍,程雪,林庭浩,等. 一维双链钙钛矿  $C_5H_{16}N_2Pb_2I_6$  的光学各向异性(特邀)[J]. 光子学报, 2023, 52(3):0352111

# 一维双链钙钛矿 $C_5H_{16}N_2Pb_2I_6$ 的光学各向异性 (特邀)

王海珍,程雪,林庭浩,李德慧

(华中科技大学 光学与电子信息学院, 武汉 430074)

**摘 要:** 研究了一维双链钙钛矿材料  $C_5H_{16}N_2Pb_2I_6$  的光学各向异性。采用水相法合成了一维双链钙钛矿  $C_5H_{16}N_2Pb_2I_6$  晶体,采用光谱对其进行表征,其荧光发射的线性二色比可达 17.4,高于已报道的一维单链  $C_4H_{14}N_2PbI_4$  钙钛矿。表明降低晶体的对称性可用于提高光学各向异性。进一步通过 Kramers-Kronig 关系获得钙钛矿的复介电常数及其双折射和二色性,其中二色性和双折射分别达到了 1.5 和 1.3。

**关键词:** 一维;双链钙钛矿;各向异性;二色性;双折射;线性二色比

中图分类号:O43

文献标识码:A

doi:10.3788/gzxb20235203.0352111

## 0 引言

偏振作为光波的基本属性之一,在先进光电子技术中起着至关重要的作用<sup>[1-3]</sup>。偏振光通常是通过利用偏振片滤除发光材料或器件的非偏振光来实现的。然而,由于在垂直于偏振方向的光被完全滤除,将导致输出光强减小至少 50%。因此,在过去的几十年里,研究具有偏振发射的发光材料引起人们广泛的关注。近年来,研究人员一直致力于新型发光材料的设计与合成,以实现高量子效率、波长可调和可控偏振发光。

利用具有各向异性的材料可以对光的偏振进行控制。晶体的光学各向异性,指沿不同方向传播的光波具有不同折射率的特性,主要是晶体微观结构对称性较低引起的。晶体结构各向异性可以导致晶体光学性质的各向异性。通常具有高光学各向异性的晶体材料具有宽带双折射、偏振选择性和大的二向色性,是制造偏振器、波片和相位匹配元件等线性和非线性光学元件的基础<sup>[4-5]</sup>。

低维层状材料的光学各向异性已经得到广泛研究。很多二维材料如黑磷<sup>[3,6]</sup>,  $GeS_2$ <sup>[7]</sup> 等由于其晶体结构的低对称性存在面内各向异性。然而大部分二维材料通常面内是光学同性的,只有面内和面外方向之间存在光学异性,大大限制了二维材料在偏振方面的应用。而一维(准一维)材料的晶体结构通常为原子排列成平行的链状结构,可以实现较大的面内各向异性<sup>[8]</sup>。并且这些刚性链沿着主轴方向,光轴处于解理面,这使得链内和链间具有很大的面内各向异性。目前虽有一维块体材料各向异性研究的报道,但因合成方法相对复杂,其光学各向异性尚未得到系统研究。此外,光电器件应用不仅要求材料具备各向异性,同时还要有其他优异的光电性质。因此,开拓具有优异光学性能和大的面内光学各向异性的材料尤为重要。

近年来,有机无机二维杂化钙钛矿材料(简称二维钙钛矿)因其优异的光学和光电性质如高量子效率、可调带隙、大的激子结合能、长扩散长度等,在太阳能电池、光电探测器和激光等方面存在潜在应用而受到广泛关注<sup>[9-13]</sup>。前期研究证实面内光学各向同性的二维(iso-BA)<sub>2</sub>PbI<sub>4</sub>钙钛矿材料面内和面外之间存在各向异性,因而可用于偏振敏感的光电探测器<sup>[6,14]</sup>。与二维钙钛矿不同,一维钙钛矿晶体因具有链状结构而具有各向异性。此外,半导体晶体结构的低对称性会进一步提高光学各向异性。因此,有望通过降低晶体结构

基金项目:国家自然科学基金(No. 62074064)

第一作者:王海珍, wanghz@hust.edu.cn

通讯作者:李德慧, dehuili@hust.edu.cn

收稿日期:2022-11-07;录用日期:2023-01-16

<http://www.photon.ac.cn>

对称性的方式来提高材料的光学各向异性。2020年,WEI Zhongming等<sup>[15]</sup>合成一种由范德华力结合的核壳结构纳米线,其各向异性明显优于单一化合物,并制备了基于此纳米线的偏振敏感光电探测器,探测范围覆盖紫外到可见光(360~532 nm)波段;且在450 nm处各向异性比可达3.14,高于很多一维材料<sup>[16-17]</sup>,证实可以通过降低对称性来提高光学各向异性。此外,本课题组前期研究也表明一维钙钛矿具有较大的光学各向异性<sup>[18]</sup>。

因此,本文旨在研究一维双链钙钛矿  $C_5H_{16}N_2Pb_2I_6$  (简称 TMEDAPb<sub>2</sub>I<sub>6</sub>) 的光学各向异性。首先采用水相法合成了一维双链的钙钛矿晶体,研究其光致发光谱(Photoluminescence, PL)的光学各向异性,并测量了其反射光谱及采用Kramers-Kronig关系(K-K关系)得到其双折射率和二色性。此研究为基于一维钙钛矿的偏振发光和光电器件的开发及性能提升奠定基础。

## 1 实验部分

### 1.1 实验药品

所用碘化铅( $PbI_2$ , 99.99%), 氢碘酸(HI, 57% w/w 水溶液)和甲胺( $CH_3NH_2$ , 40% 水溶液, MA)从Sigma Aldrich公司采购, 三甲基乙二胺( $C_5H_{14}N_2$ )采购于上海笛柏生物科技有限公司。文中采用R-NH<sub>2</sub>作为有机胺链的统称。

### 1.2 一维双链钙钛矿的合成

本文采用水相法合成一维双链钙钛矿 TMEDAPb<sub>2</sub>I<sub>6</sub> 晶体, 流程示意图如图1所示。水相法是一种在室温酸性条件下(pH<4)卤化铅和甲胺/有机链的混合溶液发生反应得到钙钛矿晶体的方法<sup>[19-20]</sup>。首先将MA和R-NH<sub>2</sub>按溶液体积3:1混合, 得到MA/R-NH<sub>2</sub>混合溶液。然后将0.05 g碘化铅粉末加入2 mL去离子水, 通过磁力搅拌得到碘化铅悬浊液, 随后加入2.5 mL氢碘酸(57% w/w)水溶液, 发生反应形成 $[PbI_4]^{2-}$ 使碘化铅溶解。进一步缓慢滴加0.6~1.4 mL MA/R-NH<sub>2</sub>(体积比3:1)的混合溶液。最后停止搅拌, 溶液自然冷却至室温, 静置后逐渐析出钙钛矿晶体。在合成过程中, 溶液中的MA<sup>+</sup>阳离子被吸附并停留在析出晶体的表面, 有利于保持溶液中的离子平衡进而利于晶体的长期稳定性。

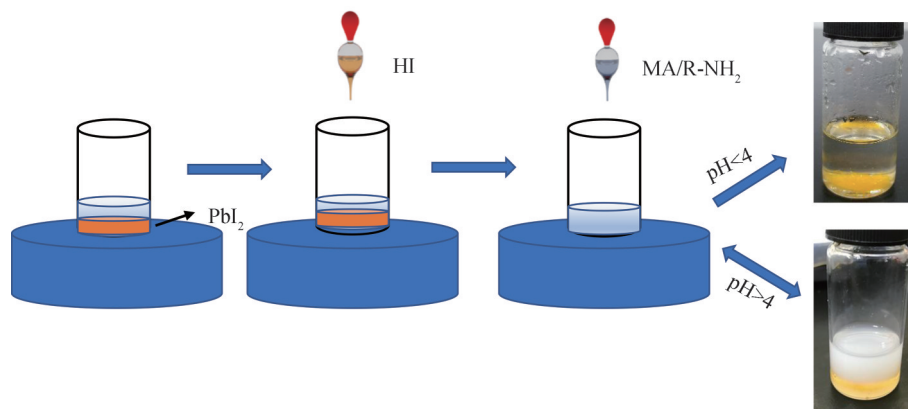


图1 水相法合成一维钙钛矿晶体的流程示意图

Fig. 1 Schematic illustration of aqueous synthesis of one-dimensional perovskites

反应产物受到溶液PH值的影响, 当加入MA/R-NH<sub>2</sub>混合溶液后, 反应溶液的pH值逐渐增加且当溶液pH值低于4时, 可以析出钙钛矿单晶。然而, 当溶液pH值超过4, 将会形成乳白色 $Pb(OH)_2$ 沉淀。当向沉淀中继续加入氢碘酸水溶液,  $Pb(OH)_2$ 将溶解使得溶液pH值降至小于4, 仍然可以析出一维钙钛矿晶体<sup>[20]</sup>。

### 1.3 样品表征

样品的晶体结构和结晶性能采用X射线衍射仪(X'pert3 powder, 荷兰帕纳科)进行测试。所得晶体的颜色大小等外观特征可以通过光学照片表征, 并采用扫描电镜(SEM, TESCAN VEGA3)测试表征所得晶体的表面形貌。钙钛矿晶体的PL光谱和反射光谱采用自制显微拉曼光谱仪(HORIBA iHR550)测量。

## 2 结果与讨论

### 2.1 一维双链钙钛矿的表征

一维双链钙钛矿  $TMEDAPb_2I_6$  晶体是基于之前报道的水相法合成的<sup>[18]</sup>,其晶体结构如图 2(a)所示。 $[PbI_4]^{2-}$ 八面体首先与两个相邻的八面体共享非共面的边缘形成一维锯齿形的链,第二条链滑动并堆叠在第一条链上。因此,该晶体具有两条八面体链,且呈现波纹状,可以看作是波纹状的一维双链结构。与一维单链钙钛矿的线性八面体链对比,此双链钙钛矿的结构对称性更低,更容易发生扭曲,各向异性可能会更大。从光学图片可以看出,采用水相法合成的一维双链钙钛矿是橙黄色针状晶体,长度大约在 2~3 mm (图 2(b))。扫描电镜照片(图 2(c))进一步显示出晶体表面微观形貌,晶体表面较光滑。一维双链钙钛矿  $TMEDAPb_2I_6$  晶体的 X 射线衍射图(XRD)如图 2(d)所示,衍射峰的峰形窄而尖锐,表明合成的钙钛矿晶体具有良好的结晶度,并且峰位与文献报道的对比后可知其为一维结构<sup>[20]</sup>。

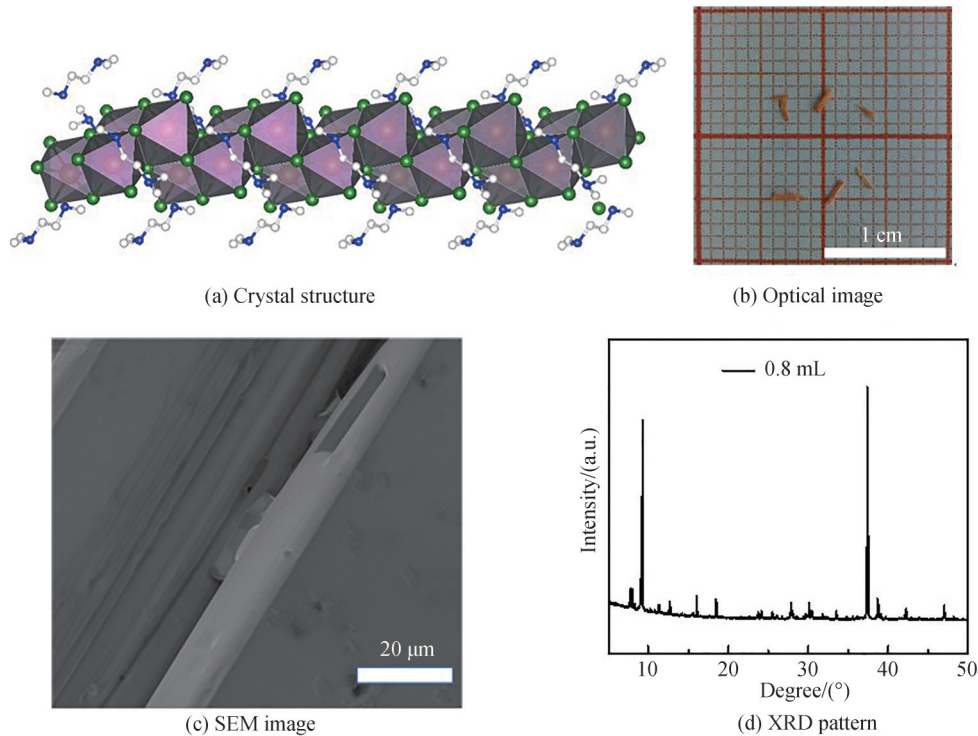


图 2 一维双链钙钛矿  $TMEDAPb_2I_6$  晶体的表征

Fig. 2 Characterizations of one-dimensional double chain  $TMEDAPb_2I_6$  perovskites

### 2.2 一维双链钙钛矿的 PL 光谱

在 78 K 下一维双链钙钛矿  $TMEDAPb_2I_6$  晶体的 PL 和吸收光谱如图 3 所示。当使用 405 nm(黑线)和 473 nm(红线)波长的激光激发样品时,其 PL 光谱均呈现两个发光峰,分别对应自陷态激子的宽带发光和自由激子的窄带发光。405 nm 光激发下的自由激子峰位于 450 nm 而 473 nm 激光激发的自由激子峰位于 500 nm 附近,这表明不同波长的激发光源下的窄带峰会发生移动且发光峰相对强度也不同,与之前一维钙钛矿的报道相吻合<sup>[21]</sup>。405 nm 波长激光激发下的 PL 谱中窄带峰强度小于宽带峰,而 473 nm 波长激光激发的 PL 谱正好相反,这表明自陷态激子更容易在 405 nm 的激光下被激发,而自由激子更容易在 473 nm 激光下被激发。这是由于不同的发射中心之间的竞争而表现出依赖于激发光的光致发光谱。钙钛矿晶体的吸收光谱峰(蓝线)出现在 400 nm 左右,而且在 700 nm 处有拖尾,表明存在多种激发态<sup>[22]</sup>。

进一步通过测量窄带峰和宽带峰发光强度随激发功率变化的关系来研究其发光机理。图 4(a)、(c)分别展示了采用波长为 405 nm 和 473 nm 的激光作为激发光源不同功率下的 PL 谱图,并通过拟合得到发光峰的强度随功率的变化关系曲线(图 4(b)、(d))。从图中可以看出,宽带峰和窄带峰的发光强度均随功率增大而增强,近似线性关系。由于缺陷和杂质的光致发光强度在强激发功率下达到饱和,因此一维双链钙钛矿

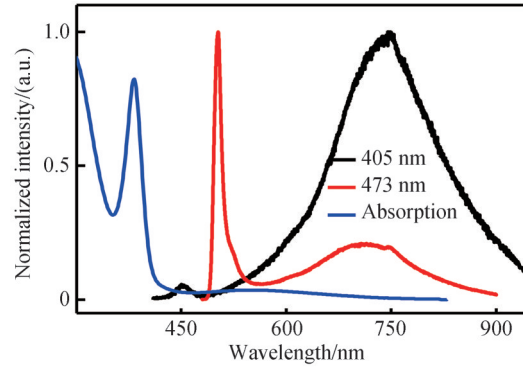


图3 78 K下一维双链钙钛矿 TMEDAPb<sub>2</sub>I<sub>6</sub> 405 nm(黑线)和473 nm(红线)激光激发下的PL光谱和吸收光谱(蓝线)  
Fig. 3 PL spectra excited by 405 nm (black line) and 473 nm (red line) laser and absorption spectrum (blue line) of one-dimensional double chain TMEDAPb<sub>2</sub>I<sub>6</sub> perovskites at 78 K

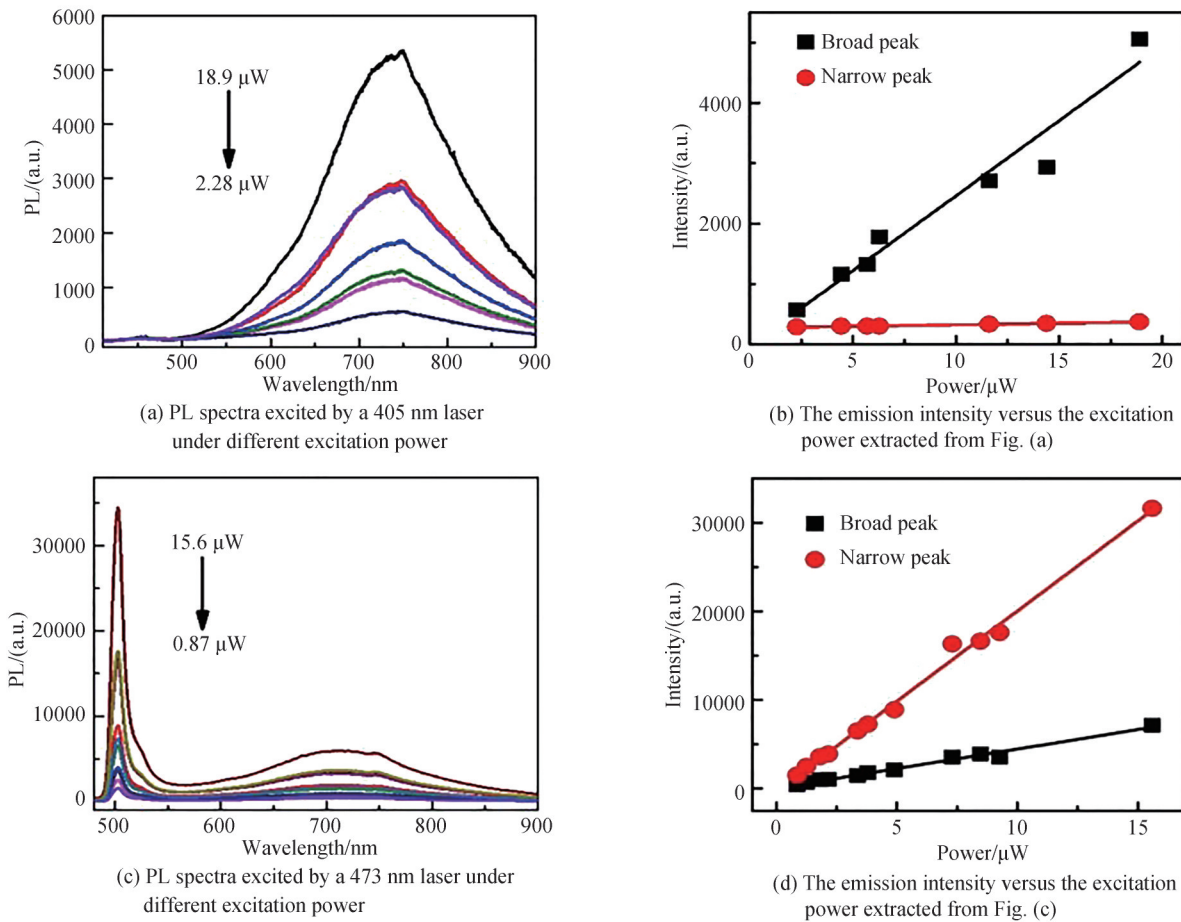
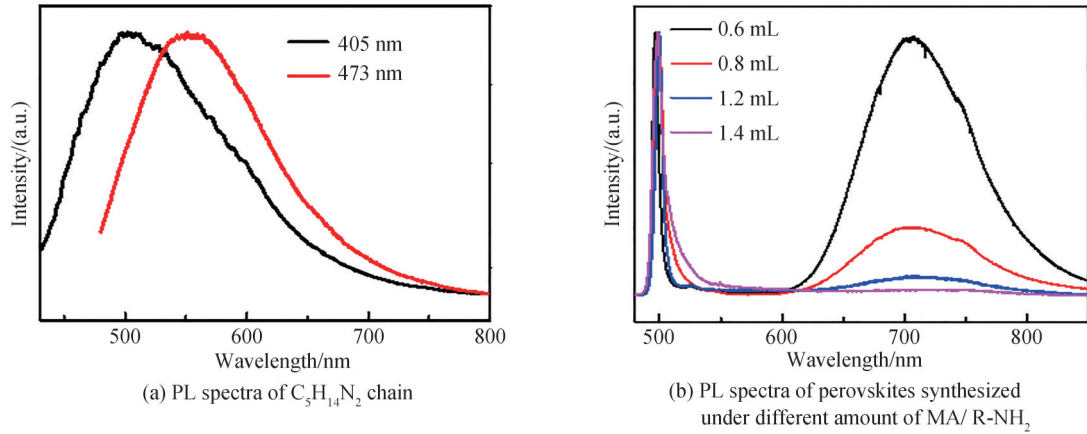


图4 一维双链钙钛矿 TMEDAPb<sub>2</sub>I<sub>6</sub> PL 光谱窄带峰和宽带峰发光强度随激发功率变化的关系  
Fig. 4 The excitation powder dependent emission intensity of one-dimensional double chain TMEDAPb<sub>2</sub>I<sub>6</sub> perovskites

的PL发光可以排除来自于缺陷和杂质发光<sup>[23]</sup>。

为了验证不同波长激光激发下一维双链钙钛矿的PL光谱窄带峰发生位移的原因,测量了有机链的PL光谱。如图5(a)所示,相比较于473 nm激光激发的光致发光峰位,405 nm激光激发下的有机链的光致发光峰位表现出明显的蓝移。此现象与一维双链钙钛矿中窄带发光峰的位移吻合,因此推测窄带峰位的移动可能由有机链C<sub>5</sub>H<sub>14</sub>N<sub>2</sub>发光导致<sup>[21]</sup>。此外,我们发现在样品合成过程中加入不同体积的有机链MA/R-NH<sub>2</sub>混合溶液会影响所得样品PL发光峰的强度。加入不同量MA/R-NH<sub>2</sub>有机链混合溶液得到的一维双链钙钛矿在473 nm激光激发下的PL谱如图5(b)所示,随着有机链MA/R-NH<sub>2</sub>混合溶液的增加,宽带峰发光强度逐

图5 有机链  $C_5H_{14}N_2$  及不同体积 MA/R-NH<sub>2</sub> 混合溶液条件下合成钙钛矿的 PL 光谱Fig. 5 PL spectra of  $C_5H_{14}N_2$  organic chain and perovskites synthesized by using different amount of MA/R-NH<sub>2</sub> solutions

渐降低。这证明了有机链的量会影响自由激子和自陷态激子的相对发光强度,可以用来调控发光器件的发光色温。

### 2.3 一维双链钙钛矿的 PL 光谱各向异性

为了研究一维双链钙钛矿的光学各向异性,采用 405 nm 波长的激光激发,测量了其 PL 光谱中自陷态激子发光各向异性,测试光路与以前采用的光路相同<sup>[18]</sup>。图 6(a)是在低温 78 K 不同偏振角度(0°, 30°和 90°)下的 PL 发射光谱,从中提取不同偏振角度下的发光强度,并使用余弦函数对数据拟合得到极坐标图如图 6(b)所示。图中呈现两瓣形状,表明一维双链钙钛矿 TMEDAPb<sub>2</sub>I<sub>6</sub>具有光学各向异性,计算得到其线性二色比( $I_{max}/I_{min}$ )为 15.9,比之前报道的一维单链钙钛矿  $C_4N_2H_{14}PbI_4$  在 78 K 的发射线性二色(1.92)提高了 7 倍<sup>[18]</sup>。这证实了通过降低晶体结构的对称性可以增强 PL 发光的各向异性。

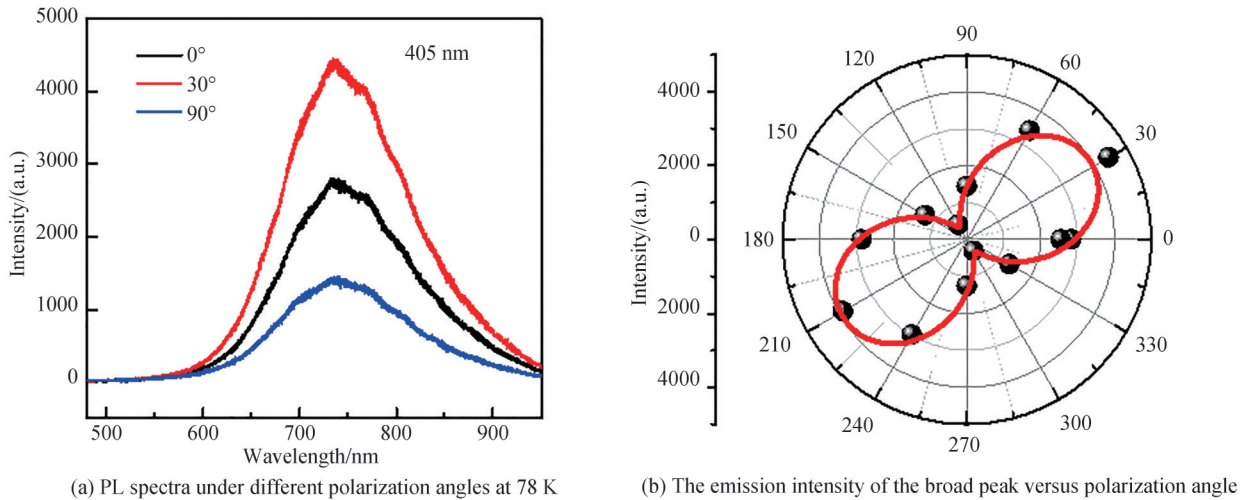


图6 78K 不同偏振角度(0°, 30°和 90°)下的 PL 光谱及 PL 强度随偏振角变化的极坐标图

Fig. 6 PL spectra under different polarization angles at 78 K and PL intensity versus polarization angles

为研究一维双链钙钛矿在不同温度下的光学各向异性,测量了不同温度下(78 K, 110 K, 140 K, 170 K, 200 K, 230 K, 260 K)的变温 PL 光谱并得到其发光强度随偏振角度变化的极坐标图。图 7 为 110 K 到 260 K (温度间隔为 30 K)的 PL 强度随偏振角度变化的极坐标图。可以明显的观测到,不同温度的极坐标图中,发光强度在偏振角度为 30°时最大,120°时最小。光致发光各向异性的大小主要由偶极简并因子和晶体结构中不同轴的电场强度决定,说明偏振角度 30°对应一维双链钙钛矿晶体的长轴<sup>[24]</sup>。

图 8 为光致发光的线性二色比随温度的变化趋势图。从图中可以看出,一维双链钙钛矿晶体的线性二色比 110 K 时最大,可达 17.4,要大于报道的一维单链钙钛矿的最大线性二色比(5.5)<sup>[18]</sup>,进一步证明通过降

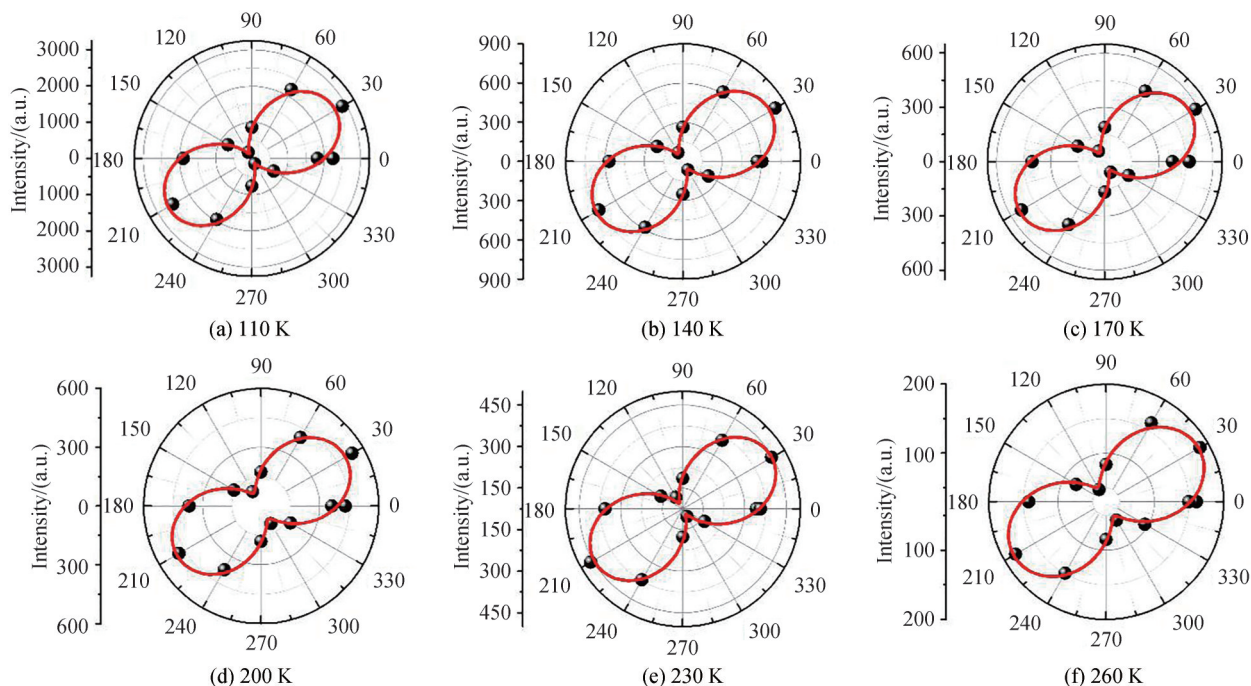


图7 405 nm 激光激发下 110 K 到 260 K 不同温度下 PL 强度随偏振角度变化的极坐标图, 温度间隔为 30 K  
Fig. 7 PL intensity versus polarization angle from 110 K to 260 K with a 30 K interval

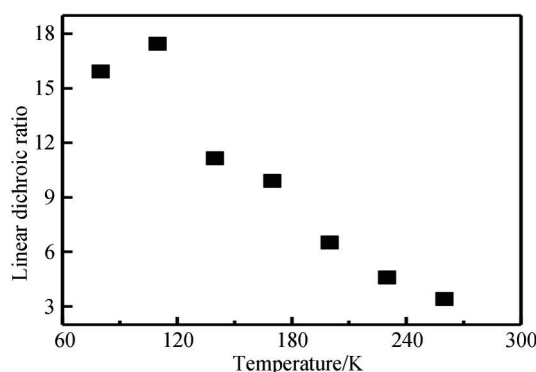


图8 78 K 到 260 K (间隔为 30 K) 温度范围内光致发光线性二色比随温度的变化  
Fig. 8 Temperature dependent linear dichroic ratio from 78 K to 260 K (30 K interval)

低晶体的对称性可以提高其光学各向异性。我们测量数个样品, 都观测到了类似的现象, 其机理有待进一步实验来厘清。此外, 线性二色比随光谱测量温度的升高而减小, 与一维单链钙钛矿的变化趋势相反, 可能由于不同方向晶格的热膨胀系数随温度升高的变化趋势与单链钙钛矿相反导致<sup>[25]</sup>。

光学各向异性可以通过各向异性材料的双折射和二色性体现, 即复折射率的实部和虚部来量化, 其主要是由晶体结构的各向异性引起的<sup>[26]</sup>。一维双链钙钛矿晶体在 290 K 下偏振角度  $0^\circ$  和  $90^\circ$  时的反射光谱如图 9(a) 所示。基于测量的反射谱, 通过 K-K 关系计算得到的晶体的折射率和消光系数如图 9(b), (c) 所示。晶体的折射率和消光系数在偏振角度为  $0^\circ$  和  $90^\circ$  时不同, 也说明一维双链钙钛矿存在光学各向异性。根据公式  $\Delta n = n_{0^\circ} - n_{90^\circ}$ ,  $\Delta k = k_{0^\circ} - k_{90^\circ}$  计算得到的双折射和二色性的大小(图 9(d))可以用于量化各向异性的大小, 其中  $n_{0^\circ}$  和  $n_{90^\circ}$ ,  $k_{0^\circ}$  和  $k_{90^\circ}$  分别为偏振方向为  $0^\circ$  和  $90^\circ$  的折射率和消光系数。在 460 nm 二色性  $\Delta k$  最大为 1.5, 而在 477 nm 双折射  $\Delta n$  达到最大值, 为 1.3。此双折射高于很多各向异性晶体的双折射, 如液晶的双折射最大只有 0.4<sup>[27]</sup>, 表明一维双链钙钛矿具有较强的光学各向异性, 在偏振发光领域具有潜在的应用前景。

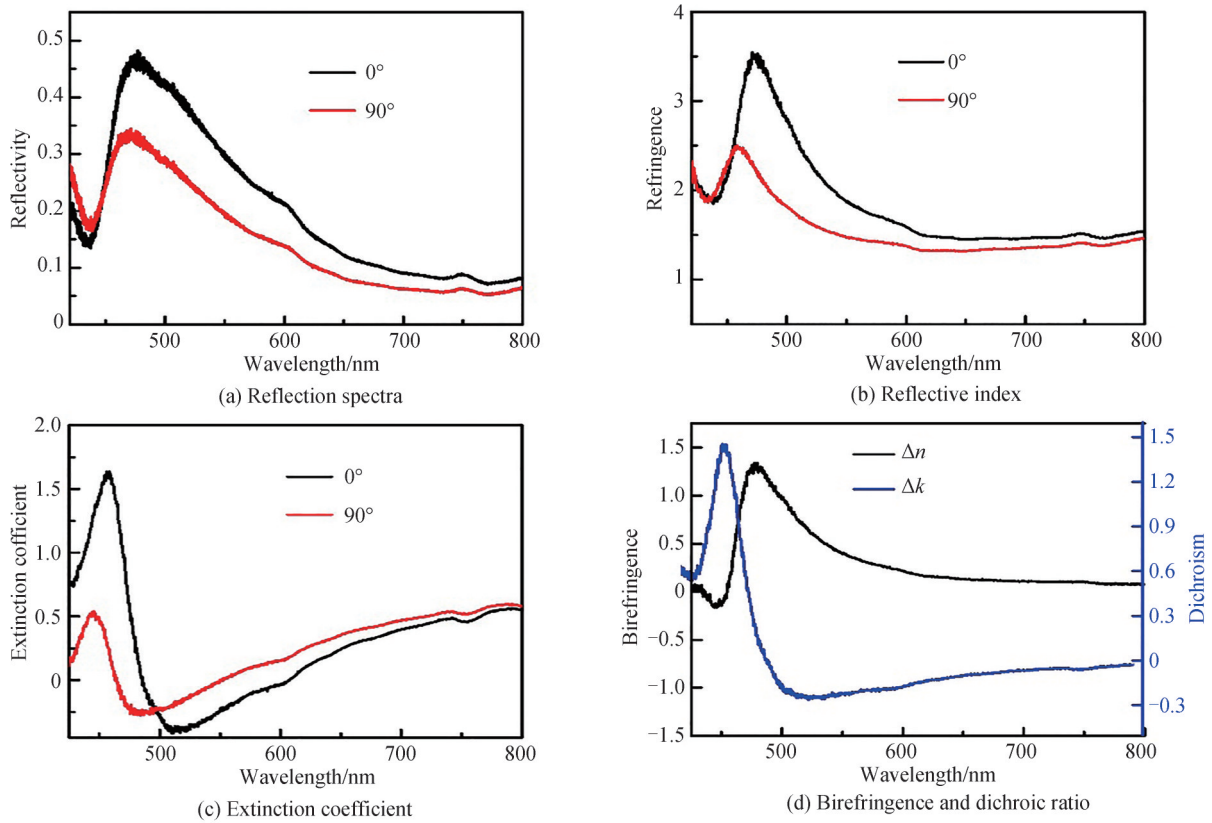


图9 偏振角度分别为  $0^\circ$  和  $90^\circ$  的 290 K 下的反射谱,利用 K-K 关系通过反射谱计算得到的一维双链钙钛矿折射率和消光系数及计算得到的双折射和二色性

Fig. 9 Reflection spectra and extracted refringence, extinction coefficient, birefringence and dichroism

### 3 结论

本文研究了一维双链钙钛矿  $C_5H_{16}N_2Pb_2I_6$  晶体的光学各向异性。采用水相法合成了一维双链钙钛矿  $C_5H_{16}N_2Pb_2I_6$  晶体,光谱表征显示其荧光发射的线性二色比达到 17.4,高于已报道的一维单链钙钛矿晶体,表明通过降低晶体的对称性可用于提高光学各向异性。进一步通过 K-K 关系计算得到一维双链钙钛矿的双折射和二色性,双折射和二色性分别达到了 1.3 和 1.5。此研究不仅证实了通过降低晶体结构的对称性提高光学各向异性的可行性,也为一维钙钛矿在偏振发光领域的应用奠定了基础。

#### 参考文献

- [1] SRIVASTAVA A K, ZHANG W, SCHNEIDER J, et al. Photoaligned nanorod enhancement films with polarized emission for liquid-crystal-display applications[J]. *Advanced Materials*, 2017, 29(33): 1701091.
- [2] WANG Y, YANG C, WANG Y, et al. Gigabit polarization division multiplexing in visible light communication[J]. *Optics Letters*, 2014, 39(7): 1823-1826.
- [3] GE Y, MENG L, BAI Z, et al. Linearly polarized photoluminescence from anisotropic perovskite nanostructures: emerging materials for display technology[J]. *Journal of Information Display*, 2019, 20(4): 181-192.
- [4] YANG H, JUSSILA H, AUTERE A, et al. Optical waveplates based on birefringence of anisotropic two-dimensional layered materials[J]. *ACS Photonics*, 2017, 4(12): 3023-3030.
- [5] WEBER M F, STOVER C A, GILBERT L R, et al. Giant birefringent optics in multilayer polymer mirrors[J]. *Science*, 2000, 287(5462): 2451-2456.
- [6] LI L, JIN L, ZHOU Y, et al. Filterless polarization-sensitive 2D perovskite narrowband photodetectors[J]. *Advanced Optical Materials*, 2019, 7(23): 1900988.
- [7] YANG Y, LIU S C, WANG X, et al. Polarization-sensitive ultraviolet photodetection of anisotropic 2D  $GeS_2$  [J]. *Advanced Functional Materials*, 2019, 29: 1900411.
- [8] NIU S, JOE G, ZHAO H, et al. Giant optical anisotropy in a quasi-one-dimensional crystal[J]. *Nature Photonics*, 2018, 12(7): 392-396.
- [9] BRENNER T M, EGGER D A, KRONIK L, et al. Hybrid organic-inorganic perovskites: low-cost semiconductors with

- intriguing charge-transport properties[J]. *Nature Reviews Materials*, 2016, 1(1): 1-16.
- [10] XING G, MATHEWS N, LIM S S, et al. Low-temperature solution-processed wavelength-tunable perovskites for lasing[J]. *Nature Materials*, 2014, 13(5): 476-480.
- [11] TAN Z K, MOGHADDAM R S, LAI M L, et al. Bright light-emitting diodes based on organometal halide perovskite[J]. *Nature Nanotechnology*, 2014, 9(9): 687-692.
- [12] LI J, WANG J, MA J, et al. Self-trapped state enabled filterless narrowband photodetections in 2D layered perovskite single crystals[J]. *Nature Communications*, 2019, 10(1): 806.
- [13] MA J, FANG C, LIANG L, et al. Full-stokes polarimeter based on chiral perovskites with chirality and large optical anisotropy[J]. *Small*, 2021, 17(47): 2103855.
- [14] LI J, MA J, CHENG X, et al. Anisotropy of excitons in two-dimensional perovskite crystals[J]. *ACS Nano*, 2020, 14(2): 2156-2161.
- [15] XIAO M, YANG H, SHEN W, et al. Symmetry-reduction enhanced polarization-sensitive photodetection in core-shell  $\text{SbI}_3/\text{Sb}_2\text{O}_3$  van der waals heterostructure[J]. *Small*, 2020, 16(7): 1907172.
- [16] XIA J, ZHU D, LI X, et al. Epitaxy of layered orthorhombic  $\text{SnS}-\text{SnS}_2\text{Se}_{(1-x)}$  core-shell heterostructures with anisotropic photoresponse[J]. *Advanced Functional Materials*, 2016, 26(26): 4673-4679.
- [17] YANG H, PAN L, WANG X, et al. Mixed-valence-driven quasi-1D  $\text{SnIISnIVS}_3$  with highly polarization-sensitive UV-vis-NIR photoresponse[J]. *Advanced Functional Materials*, 2019, 29(38): 1904416.
- [18] CHENG X, MA J, ZHOU Y, et al. Optical anisotropy of one-dimensional perovskite  $\text{C}_4\text{N}_2\text{H}_{14}\text{PbI}_4$  crystals[J]. *Journal of Physics: Photonics*, 2020, 2(1): 014008.
- [19] GENG C, XU S, ZHONG H, et al. Aqueous synthesis of methylammonium lead halide perovskite nanocrystals[J]. *Angewandte Chemie International Edition*, 2018, 57(31): 9650-9654.
- [20] WANG J, FANG C, MA J, et al. Aqueous synthesis of low-dimensional lead halide perovskites for room-temperature circularly polarized light emission and detection[J]. *ACS Nano*, 2019, 13(8): 9473-9481.
- [21] PENG Y, YAO Y, LI L, et al. White-light emission in a chiral one-dimensional organic-inorganic hybrid perovskite[J]. *Journal of Materials Chemistry C*, 2018, 6(22): 6033-6037.
- [22] ZHANG Y, YIN J, PARIDA M R, et al. Direct-indirect nature of the bandgap in lead-free perovskite nanocrystals[J]. *The Journal of Physical Chemistry Letters*, 2017, 8(14): 3173-3177.
- [23] ZHOU B, LIANG L, MA J, et al. Thermally assisted rashba splitting and circular photogalvanic effect in aqueously synthesized 2D dion-jacobson perovskite crystals[J]. *Nano Letters*, 2021, 21(11): 4584-4591.
- [24] MA X, DIROLL B T, CHO W, et al. Anisotropic photoluminescence from isotropic optical transition dipoles in semiconductor nanoplatelets[J]. *Nano Letters*, 2018, 18(8): 4647-4652.
- [25] ZHANG Zhaojun, ZHENG Wei, WANG Weiliang, et al. Anisotropic temperature-dependence of optical phonons in layered  $\text{PbI}_2$  [J]. *Journal of Raman Spectroscopy*, 2018, 49(4): 775-779.
- [26] YUAN H, LIU X, AFSHINMANESH F, et al. Polarization-sensitive broadband photodetector using a black phosphorus vertical p-n junction[J]. *Nature Nanotechnology*, 2015, 10(8): 707-713.
- [27] HERMAN J, KULA P. Design of new super-high birefringent isothiocyanato bistolanes-synthesis and properties [J]. *Liquid Crystals*, 2017, 44(1462): 1467.

## Optical Anisotropy of One-dimensional Double Chain $\text{C}_5\text{H}_{16}\text{N}_2\text{Pb}_2\text{I}_6$ Perovskites (Invited)

WANG Haizhen, CHENG Xue, LIN Tinghao, LI Dehui

(School of Optical and Electronic Information, Huazhong University of Science and Technology, Wuhan 430074, China)

**Abstract:** In addition to amplitude, frequency and phase, the polarization states of light can also carry information and thus will find important applications in imaging, medical detection and optical communication. Traditionally, the generation and detection of polarized light mainly rely on the combination of commercial unpolarized light sources and photodetectors with polarizer and wave plate, which are usually bulky and costly. Therefore, it is urgent to develop alternative strategies to achieve on-chip compact polarized light source and detector. Optical anisotropy is related to the polarization response of optoelectronic devices, which is the basis for polarization optical elements such as polarizers, wave plates,



and phase matching devices. The study on the optical anisotropy is of great significance for polarization-sensitive photodetectors and light emitting devices. In recent years, perovskites have received extensive attention due to their prominent optoelectronic properties and potential applications in optoelectronic devices. In particular, one dimensional perovskites are expect to exhibit large optical anisotropy due to the crystalline structure anisotropy. Together with the excellent optoelectronic properties of perovskites, we anticipate that one dimensional perovskites will find promising potential applications in the polarization-resolved optics. However, its optical anisotropy has been rarely reported. Our previous study has reported on the optical anisotropy of one-dimensional single chain perovskites, which exhibits a large emission linear dichroic ratio of 5.5 at room temperature. Nevertheless, this linear dichroic ratio is still not large enough for certain polarization resolved applications and far smaller than the linear dichroic ratio of the commercial optical elements. In this end, it is necessary to explore new materials to enhance the optical anisotropy.

According to previous reports, it is possible to further increase the optical anisotropy by reducing the symmetry of the crystalline structure of a materials. By reducing the symmetry of the crystal structure, the octahedral structure of perovskites is more prone to distort, which increases the anisotropy of the transition dipole moment, thus increasing the optical anisotropy. Based on this principle, we design a one dimensional double chain perovskites, which will have a much lower symmetry compared with one dimensional one chain perovskites and thus can possibly exhibit a much larger optical anisotropy. The single crystal of one dimensional double chain perovskite  $C_5H_{16}N_2Pb_2I_6$  crystals are synthesized via aqueous synthesis route. The as-synthesized crystals show needle-like shape with a length of 2~3 mm. X-ray diffraction pattern reveals the excellent crystal quality and one-dimensional nature of the crystals. Scanning microscope images show that the crystals have a rather smooth surface, which is beneficial for the spectroscopic measurement. The photoluminescence (PL) spectra of the as-synthesized crystals suggest that the spectral profile strongly depends on the excitation laser. Under a 405 nm laser excitation, the PL spectrum has a strong narrow emission peak at the high energy side and a weak broad emission peak at the low energy side while the spectrum is dominated by the broad emission peak when excited by a 473 nm laser. Nevertheless, both of those two emission peak show a linearly increase with the increasing the excitation power, which can exclude that those emission peaks are from defects or impurities. Together with previous studies, we assigne those two emission peaks as free exciton emission and self-trapped exciton emission. Since the broad emission can find important applications in white light emitting devices, we focus on the optical anisotropy of the broad emission peak hereafter.

The temperature dependent polarization resolved PL studies have been carried out from 78 K to 260 K. For all temperature range we have investigated, a large optical anisotropy of PL spectra has been observed. At 78 K, the linear dichroic ratio can reach about 15.9, which is 7 times larger than that in a one dimensional single chain perovskite crystals (1.92). This observation confirms our hypothesis that reducing the symmetry of the crystalline structure of a material can indeed improve the optical anisotropy. The maximum linear dichroic ratio of our crystals appears at 110 K, which can be as large as 17.4, and also much larger than the maximum linear dichroic ratio in one dimensional single chain perovskite crystals (5.5). Finally, we have also extracted the complex dielectric constant, birefringence and dichroism of our crystals based on the reflection spectra via Kramers-Kronig relation. The birefringence and linear dichroic ratio reflect the real and imaginary part of complex dielectric constant, which are intrinsic properties of a materials and originated from the optical anisotropy of a material. The extracted dichroism and birefringence can reach 1.5 and 1.3, respectively. The birefringence of our crystals is much larger than the highest values reported in liquid crystals. In summary, the optical anisotropy of one-dimensional double chain perovskite crystals has been systematically studied, and the optical anisotropy of the crystals is proven to be improved by reducing the symmetry of crystals. Our study is of great significance for polarization sensitive optoelectronic devices based on one-dimensional double chain perovskites and shed light on how to further improve the optical anisotropy via deigning the crystal structure of a material.

**Key words:** One-dimensional; Double chain perovskites; Optical anisotropy; Dichroism; Birefringence; Linear dichroic ratio

**OCIS Codes:** 160.1190; 300.6280; 300.6470; 260.5430